

XPS ANALYSIS OF THIN INSULATING BARRIERS IN MAGNETIC TUNNEL JUNCTIONS

X. BATLLE*, B. J. HATTINK, A. LABARTA
*Dept. Fisica Fonamental, Universitat Barcelona,
Av. Diagonal 647, 08028, Barcelona, Catalonia, Spain*
B. J. JÖNSSON-ÅKERMAN, R. ESCUDERO, I. K. SCHULLER
*Physics Department-0319, U. California – San Diego
9500 Gilman Drive, La Jolla, CA 92093, US*

Large efforts have been lately devoted to the study of the structural, magnetic and transport properties of magnetic tunnel junctions (MTJ) [1] due to their potential applications as low magnetic field sensors and magnetic random access memories. MTJ are based on trilayered systems of the type FM1/I/FM2, where FM1 and FM2 are ferromagnetic electrodes and I is a thin insulating barrier (1-3 nm in thickness). Much research have been undertaken on insulating barriers based on an Al layer which is oxidized either after being deposited (e.g., by natural or plasma oxidation) or while being deposited (e.g., by reactive sputtering). The technological needs for the application of MTJ are strongly dependent on the thickness and surface roughness of the Al layer, as well as on its oxidation, which has to be uniform and complete (without pinholes).

X-ray photoelectron spectroscopy (XPS) [2] is an excellent technique for the analysis of thin insulating barriers. XPS displays an energy resolution that allows to study the chemical species in the sample as well as the bonding state (either metallic or insulating) of a given element. This is suitable for the analysis of the relative AlO_x -Al ratio, which governs the transport properties of the MTJ. Besides, the spatial resolution depends on two facts: (1) the XPS signal averages the number of out-coming electrons from a region of about 5-10 nm in depth from the sample surface, and (2) the sample is usually ion beam sputtered (4 keV, incident at 45°) in order to obtain a depth profile. We present here an XPS analysis of Nb/Al wedge bilayers, oxidized by glow discharge and natural oxidation. We will discuss, among other things, the AlO_x -Al chemical shift and the oxidation state of the former, as functions of the oxidation method.

Nb (100 nm)/Al bilayers were dc sputtered onto Si substrates. The nominal thickness of the wedge Al layer ranged within 4 nm (thinnest area) and 8 nm (thickest area). Sample W_{AIR} was exposed to ambient air for about two months. Sample W_{PLASMA} was glow discharged ($p_{\text{O}_2} = 350$ mTorr, 350 V dc bias) for 2.3 hours. XPS intensities of the O $1s$, Nb $3d_{5/2}$ and $3d_{3/2}$, and Al $2p$ photoelectron lines were recorded using the Al K_{α} emission line, for W_{AIR} and W_{PLASMA} in both the thinnest and thickest areas of the wedge. We will refer to them as $W_{\text{AIR}}(t_{\text{Al}} = 4 \text{ nm})$, $W_{\text{AIR}}(t_{\text{Al}} = 8 \text{ nm})$, $W_{\text{PLASMA}}(t_{\text{Al}} = 4 \text{ nm})$ and $W_{\text{PLASMA}}(t_{\text{Al}} = 8 \text{ nm})$. Depth profiles were obtained as follows: step 1 is the

surface spectrum, step 2 is the spectrum after sputtering for 18 s, so that step n is spectrum after sputtering for $18 \times (n - 1)$ s.

Figure 1(a) shows the atomic concentration obtained from the XPS intensities [2] for (Al+AlO_x), O, Nb, C and Ar, as a function of the sputtering step (and time), for sample W_{AIR} ($t_{Al} = 8$ nm). Figures 1(b), 1(c) and 1(d) show the spectra for (Al + AlO_x), O and Nb, respectively, for the same sample. Numbers indicate the sputtering step. Figure 2 displays the depth profiles obtained from the fitted intensities of the Al and AlO_x contributions to the (Al + AlO_x) spectra (Figure 1(b)), for all four samples.

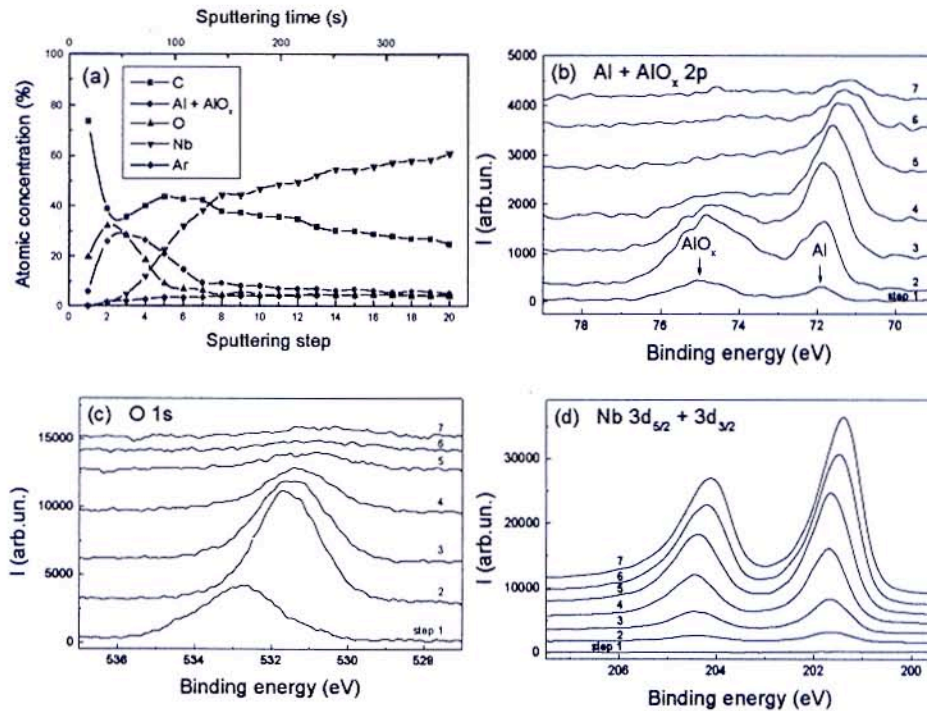


Figure 1. Sample W_{AIR} ($t_{Al} = 8$ nm): (a) Atomic concentration obtained from the XPS intensities for (Al + AlO_x), O, Nb, C and Ar, as a function of sputtering step (and time). (b) XPS spectra for (Al + AlO_x) 2p lines, (c) spectra for O 1s line, and (d) spectra for Nb (3d_{5/2} + 3d_{3/2}) lines. Numbers indicate sputtering step.

The main general results (Figure 1) are the following: (i) no Nb-O compound is detectable for any sample, while there is a non-oxidized Al leftover for all them, as expected taking into account the Al thickness [3-5], and (ii) C contamination is evident for all samples oxidized in air, which is not the case for glow discharged ones (not shown).

The thickness of the AlO_x layer, $t(\text{AlO}_x)$, may be evaluated through the expression $t(\text{AlO}_x) = \lambda(\text{Al}) \sin\theta \ln(R/K + 1)$ [2], where $\lambda(\text{Al}) = 3 \times [\text{KE}/1386]^{0.72} = 3.04$ nm is the mean free path for Al 2p electrons, $\sin\theta$ is a geometrical factor ($\theta = 45^\circ$),

$R=I(\text{AlO}_x)/I(\text{Al})$ is the intensity ratio in step 1 (surface spectra) and $K = \rho(\text{AlO}_x)/\rho(\text{Al})$ is the ratio of densities. This expression applies when $t_{\text{Al}} \geq 3\lambda(\text{Al})$ [2], which is the case for those two samples with $t_{\text{Al}} = 8$ nm, and it yields $t(\text{AlO}_x) = 2.8$ nm for $W_{\text{AIR}} (t_{\text{Al}} = 8$ nm) and $t(\text{AlO}_x) = 2.1$ nm for $W_{\text{PLASMA}} (t_{\text{Al}} = 8$ nm). Consequently, the AlO_x surface layer seems to be thicker for natural oxidation.

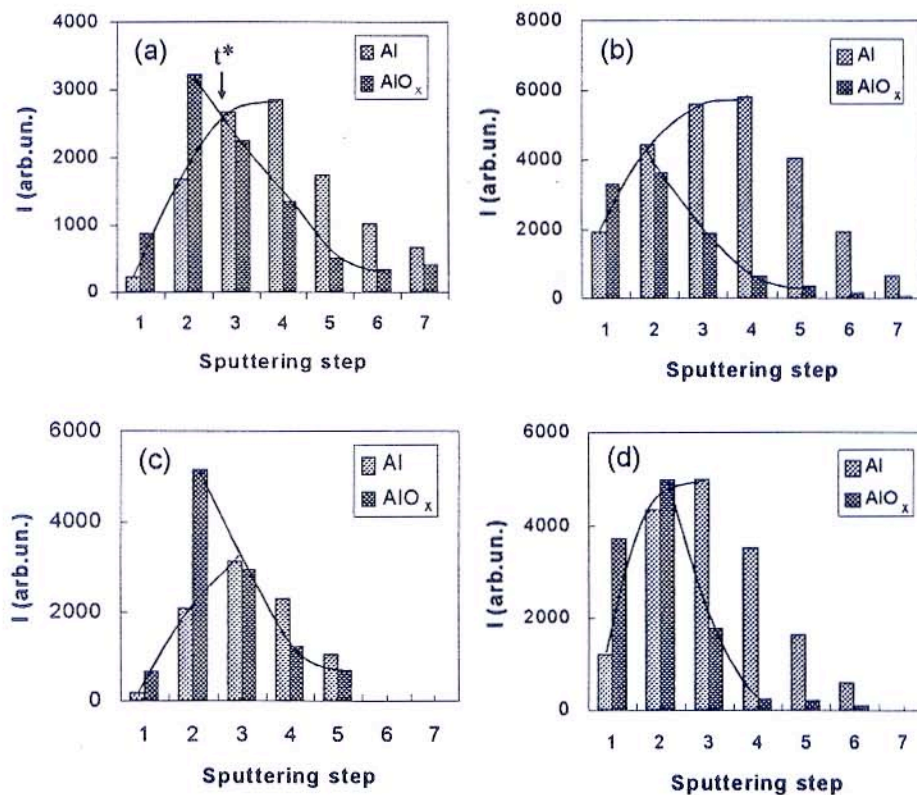


Figure 2. Depth profile showing the fitted intensities of the Al and AlO_x contributions to the $(\text{Al} + \text{AlO}_x)$ spectra in Figure 1(b), for samples (a) $W_{\text{AIR}} (t_{\text{Al}} = 8$ nm), (b) $W_{\text{PLASMA}} (t_{\text{Al}} = 8$ nm), (c) $W_{\text{AIR}} (t_{\text{Al}} = 4$ nm), and (d) $W_{\text{PLASMA}} (t_{\text{Al}} = 4$ nm). t^* indicates the sputtering time for which $I(\text{AlO}_x) = I(\text{Al})$.

Once $t(\text{AlO}_x)$ is determined, the sputtering rate (SPR) can be evaluated as $\text{SPR} = t(\text{AlO}_x) / t^*$, where t^* is the time for which $I(\text{AlO}_x) = I(\text{Al})$ (see Figure 2). t^* is larger for natural oxidation and leads to $\text{SPR} = 4.7$ nm/minute for $W_{\text{AIR}} (t_{\text{Al}} = 8$ nm) and $\text{SPR} \approx 9.5$ nm/minute for $W_{\text{PLASMA}} (t_{\text{Al}} = 8$ nm), although $t^* \approx 13$ s for the latter, thus meaning that t^* is within step 1 and 2, so that the amplitude of the sputtering step (18 s) should be reduced in further XPS experiments. Typical values of SPR are 9.4 nm/minute for SiO_2 and 6.0 nm/minute for TiO_2 . We note that SPR depends on both the structure of the AlO_x layer and the surface contamination, the latter being also dependent on the former (see below). Finally, by using SPR and t^* , we estimate $t(\text{AlO}_x) \approx 2.8$ nm for $W_{\text{AIR}} (t_{\text{Al}} = 4$ nm).

XPS may also give an estimate of the O : (oxidized) Al ratio. This ratio is computed in step 2 (after cleaning the sample surface) for samples W_{AIR} . We cannot evaluate it for W_{PLASMA} since t^* already corresponds to about step 2. By taking into account the dependence of the experimental XPS intensity on the thickness of the layers [2-3] and the scattering cross section for photoelectrons [2], we obtain O: Al \approx 1.8 – 1.9 for W_{AIR} ($t_{\text{Al}} = 4$ nm) and O: Al \approx 2.0 for W_{AIR} ($t_{\text{Al}} = 8$ nm), thus suggesting that natural oxidation leads to both AlOOH and Al₂O₃ at the surface layer.

In conclusion, as native oxides of transition metals obtained by natural oxidation in air are hydrophilic and porous at the sample surface, O₂ may easily diffuse and this is probably the reason why the oxide layer is thicker than for glow discharged samples. Native oxides also show poor insulating properties and they generally form oxide-hydroxide surface compounds (e.g., AlOOH), so that a thick surface contamination layer adds to the sample, as evidenced in Figure 2 (the intensity in step 1 for natural oxidation is much smaller than in step 2, which is not the case for glow discharge). On the contrary, 'artificial' oxidation, e.g., glow discharge, leads to a more compact and thinner surface oxide layer, probably close to the expected O/Al:1.5 value [4]. This layer acts as a passivation layer: as it grows more compact, it avoids further O₂ diffusion. Consequently, the surface layer of contamination is also thinner since the C-H and O-H groups cannot add to the surface so easily (Figure 2), and the sputtering rate during the first steps is higher.

Acknowledgements

XB is indebted to Drs. J. Portillo and J.L. Alay for their technical support during the XPS experiments and because of many fruitful discussion of data. Financial support of the Spanish CICYT through the MAT97-0404 project and the Generalitat de Catalunya through the ACI98-14 Joint Action are gratefully recognized.

References

1. Moodera, J.S., et al. (1995) Large magnetoresistance at room temperature in ferromagnetic thin film tunnel junctions, *Physical Review Letters* 74, 3273-3276.
2. see for example, (1983) D. Briggs and M.P. Seah (eds.), *Practical Surface Analysis*, John Wiley & Sons Ltd., Chichester.
3. Battle, X., Hattink, B.J., Labarta, A., Jönsson-Akerman, B.J., Escudero, R., and Schuller, I.K., to be published.
4. LeClair, P. et al. (2000) Optical and in situ characterization of plasma oxidized Al for magnetic tunnel junctions, *Journal of Applied Physics* 87, 6070- 6072.
5. de Gronckel, H.A.M. et al (2000) Pre-requisites for high-quality magnetic tunnel junctions: XPS and NRM study of Co/Al bilayers, *Appl. Phys. A* 70, 435-441.

* Author for correspondence: xavier@ffn.ub.es